Journal of nanoporous Systems

Original Research Paper

Theoretical investigation on the possible deactivation of the pollutant benzo[α]pyrene by C_{20} fullerene through a cycloaddition reaction

Reza Khazaeinejad

Education Administration, Daran, Isfahan, Iran

Article history
Received: 20 January 2025
Revised: 14 March 2025
Accepted: 11 April 2025

*Corresponding Author:
Reza Khazaeinejad,
Education Administration,
Daran, Isfahan, Iran;
Email:
khazaei6399@gmail.com

Abstract: Benzo[α]pyrene is one of the polycyclic aromatic hydrocarbon compounds present in the atmosphere, produced through the incomplete combustion of fossil fuels, and is a known carcinogen. This study investigates the potential deactivation of benzo[α]pyrene through a reaction with C_{20} fullerene using quantum computational methods. For this purpose, the thermodynamic and kinetic parameters of the [4+2] reaction between benzo[α]pyrene and fullerene were calculated. The results showed that this reaction is thermodynamically favorable with negative enthalpy and free energy. Kinetically, it occurs with a rate constant of 9.24×10^{-5} s^{-1} at a temperature of $25^{\circ}C$. Using Fukui functions, the active sites of benzo[α]pyrene for the reaction were identified. The effective orbital for the FERMO reaction of this molecule was also determined. This orbital is located at an energy level of -0.2564 a.u., where the contributions from the active site atoms (atoms 1 and 4) are maximized and can interact with the LUMO orbital of fullerene. The results from the General Electron Density Transfer (GEDT) calculations indicated that in this reaction, an electron is transferred from benzo[α]pyrene to fullerene, and the reaction exhibits some polar character. Finally, the calculations of reaction synchrony showed a low degree of synchrony, indicating that the progress of forming two bonds between fullerene and benzo[α]pyrene in the transition state is not identical.

Keywords: C_{20} fullerene, benzo[α]pyrene, cycloaddition reaction, Fukui functions, FERMO

Introduction

Polycyclic aromatic hydrocarbons (PAHs) are compounds consisting of two or more fused aromatic rings that exist in various forms. These compounds are often found in the environment as mixtures and are not seen in isolation. Some examples of PAHs include naphthalene, anthracene, fluoranthene, phenanthrene, pyrene, benzo[α]pyrene, benzo[k]fluoranthene, and others. PAHs are a significant group of environmental carcinogens that are found everywhere as pollutants in water, air, and soil, and they pose health risks due to their persistence and stability in different environments. These substances arise from natural events such as forest fires, volcanic activities, as well as from the incomplete combustion of fossil fuels, metallurgical processes, and so forth, leading to their widespread distribution in the environment. Apart from the small amounts productions that produced from geochemical and natural sources, polycyclic aromatic hydrocarbons are primarily derived from human activities. Industrial smokestacks, automobile exhausts, incinerators, and residential heating devices are major sources of PAH air pollution. Oil-related pollution is also noteworthy, which can occur due to oil pipeline ruptures, tank deterioration, leaks from aboveground or even underground storage tanks, and various other incidents that typically occur during the production and transportation of petroleum products. Furthermore, this pollution can occur naturally due to the seepage of oil from underground oil and gas reservoirs to the surface [1,2]. Due to the presence of π-systems in polycyclic aromatic compounds, cycloaddition reactions can be one of their important reactions [3]. In these reactions, two or more unsaturated compounds react to form a cyclic compound. The Diels-Alder reaction is one of the most important cycloaddition reactions that can occur both intermolecularly and intramolecularly. This reaction is a [4+2] reaction that often proceeds through a concerted mechanism [4,5].

Fullerenes are a class of carbon nanostructures that exist in spherical, elliptical, or tubular forms composed of π-bonds. These molecules, like carbon nanotubes, have considerable potential for applications in medicine and nanotechnology [6,7]. Due to the presence of conjugated π-systems, fullerenes can undergo cycloaddition reactions with other π-containing compounds [8]. Among fullerenes, C_{20} is the smallest possible fullerene, consisting of only 12 carbon pentagons. The smallest fullerene, C_{20}, was firstly synthesized using $C_{20}H_{20}$ which was converted to $C_{20}Br_{20}$ and then brominated in the gas phase [9], after that characterized by photoelectron technique [10]. According to its cyclic aromaticity, low energy gap, and inherent instability that make it reactive, the cycloaddition reaction of this fullerene with other π-systems can be intriguing. The reaction of fullerene C_{60} with certain π-systems has been reported, including reactions with naphthalene [11], acenes [12], and substituted anthracene derivatives at position 9 [8]. Theoretical studies on the functionalization of fullerenes with certain π-systems have also been reported, such as the reaction of C_{60} with 3,2-dimethylen-4,1-dioxane and 5,2-dioxabicyclo [4.2.0]octa-1(8),6-diene [13], C_{20} with pyrene, ketene, pyridine and pyrimidine [14-16].

Since theoretical calculations can facilitate experimental studies and confirm them, the present research investigates the possibility of the [4+2] reaction between fullerene C_{20} and benzo[α]pyrene as a pollutant from a theoretical perspective. One of the objectives of this study is to explore the potential for trapping benzo[α]pyrene by this fullerene nanostructure.

Materials and Methods

Calculations were performed using the G09 software package [17]. The calculations were conducted using the B3LYP method with the 6-311G* basis set [18]. Using the optimized structure of the reactants and products, the transition state (TS) for each reaction was determined. IRC calculations confirmed the TS structures [19]. Additionally, frequency calculations indicated that each transition state has one and only one imaginary frequency corresponding to bond formation.

The reaction rate constant was obtained using the Arrhenius equation:

$$k = (\frac{K_B T}{h}) \exp(\frac{-\Delta G^{\#}}{RT})$$

where k is the reaction rate constant, K_B is the Boltzmann constant, T is the temperature in Kelvin, h is Planck's constant, $\Delta G^{\ddagger}$ is the free energy of activation, and R is the gas constant [20].

The synchrony (Sy) of the reactions was calculated using the following equation [21]:

$$s_y = 1 - \frac{1}{2n-2} \sum \frac{[\delta B_i - \delta B_{av}]}{\delta B_{av}}$$

where δB_i is the relative change in bond order in the transition state, δB_{av} is a measure of the progress of the transition state during the reaction, and n is the number of bonds that directly participate in the reaction. Based on the value of *Sy*, reactions can be classified as stepwise reactions at *Sy*=0 and synchronous reactions at *Sy*=1, with varying degrees of synchrony depending on the *Sy* value.

Using the NBO method, the electric charges on the atoms in the reactants, transition state structures, and products were calculated [22]. The electrophilicity index (ω) was calculated using the following equation:

$$\omega = \frac{\mu^2}{2\eta}$$

where μ and η are the chemical potential and chemical hardness, respectively [23].

Results and Discussions

In the previous reported cycloaddition reactions involving fullerenes, the Diels-Alder reaction has been noted, where the fullerene acts as a dienophile and the π-systems that serve as the diene [11, 12, 14-16]. In this study, a similar [4+2] reaction was considered, in which the fullerene and benzo[α]pyrene act as the dienophile and diene, respectively. Figure 1 illustrates the proposed reaction along with atom numbering. In this reaction, benzo[α]pyrene reacts with the fullerene at positions 1 and 4.

Subsequently, each of the above structures was optimized using the B3LYP/6-311G** computational method.

DFT indices are powerful tools for explaining reactivity and regioselectivity in organic polar reactions [24]. Therefore, these indices including electronic chemical potential (*μ*), chemical hardness (*η*), global electrophilicity (*ω*), and global nucleophilicity (*N*) were calculated for benzo[α]pyrene as well as for fullerene C_{20} in *eV*. Table 1 indicates the summary of the above mentioned parameters.

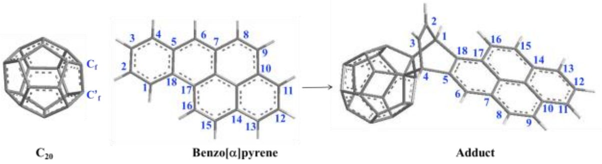

Fig. 1. [4+2] Reaction between Fullerene C_{20} and Benzo [α] pyrene.

Table 1. DFT Indices for Benzo[α]pyrene and Fullerene C_{20} in *eV*.

Species	μ	η	ω	N
benzo[α]pyrene	-3.68	1.68	4.03	4.00

C_{20}	-4.48	0.97	10.34	3.92

The results in Table 1 indicate that the electron chemical potential of fullerene C_{20} is lower than that of benzo[α]pyrene. The electrophilicity index also suggests that fullerene possesses a significant electrophilicity, allowing it to act as an electron acceptor. Therefore, it can be expected that during the related cycloaddition reaction, electrons will be transferred from benzo[α]pyrene to fullerene. Overall, it can be concluded that in the proposed reaction, fullerene acts as an electron acceptor while benzo[α]pyrene acts as an electron donor.

To investigate the kinetics, the transition state of the cycloaddition reaction between fullerene C_{20} and benzo[α]pyrene was determined using the B3LYP/6-311G** method. Figure 2 illustrates the optimized structure of this transition state along with its imaginary frequency, as well as the optimized structures of the reactants and product. The observed transition state features exactly one imaginary frequency corresponding to bond formation, and its IRC calculations have confirmed this.

Next, using the results from the optimization calculations of the reactants, transition states, and products, the energy E, enthalpy H, entropy S, and Gibbs free energy G were determined. Additionally, the relative energies ΔE, relative enthalpies ΔH, relative entropies ΔS, and relative Gibbs free energies ΔG were calculated with respect to the reactants as the baseline. In other words, the relative change in each parameter was computed by subtracting the corresponding value of the transition state or product from that of the reactants. The results are presented in Table 2.

Figure 3 shows the relative changes in total energy ΔE along with the changes in Gibbs free energy ΔG as a function of reaction progress.

With the activation free energy determined, the reaction rate constant was also calculated using the Arrhenius equation, yielding a value of $9.24\times10^{-5}\,s^{-1}$ at a temperature of 25°C.

An examination of the data in Table 2 and the diagrams in Figure 3 reveals that:

1. As the reaction proceeds, the entropy of the reactants decreases due to the reduction in the degrees of freedom.
2. The reaction has favorable thermodynamic conditions, and the product is more stable than the reactants, as confirmed by the energy, enthalpy, and free energy data.

In polar reactions involving asymmetric reactants, when the electrophile and nucleophile approach each other, the most likely event involves the interaction between the electrophilic center and the nucleophilic center. One parameter that can be used to analyze reactivity is Fukui functions [25]. These functions are proposed based on the molecular charges within a molecule:

$f_k^- = q_k(N) - q_k(N-1)$ for electrophilic attack
$f_k^+ = q_k(N+1) - q_k(N)$ for nucleophilic attack

Fukui functions are capable to determine certain reactivity indices, such as electrophilicity and nucleophilicity associated with an atom in a molecule, and consequently identify the most electrophilic and nucleophilic centers of a reactant [26, 27].

$\omega_k = \omega f_k^+$ local electrophilicity
$N_k = N f_k^-$ local nucleophilicity

These functions are suitable to assess regioselectivity. In cycloaddition reactions, the most favorable interaction involves the strongest electrophilicity and local nucleophilicity. Therefore, to study this reaction, the Fukui functions were calculated. Since in the reaction of interest, benzo[α]pyrene acts as an electron donor (or nucleophile), f_k was calculated for it, and this parameter allowed the determination of the local nucleophilicity at various sites on benzo[α]pyrene. The calculated local nucleophilicity for benzo[α]pyrene is shown in Figure 4. According to Figure 4, carbon atoms 1, 3, 4, 6, 8, 9, 11, 13, 15, and 16 show higher nucleophilicity (as numbered in Figure 1). In the [4+2] cycloaddition reaction, benzo[α]pyrene acts as a diene, and the two atoms at positions 1 and 4 must participate in the reaction, necessitating that these two atoms exhibit high nucleophilicity. From the results in Figure 4, it can be concluded that both 1 and 4 carbon atoms are activated more nucleophilically. Thus, based on these calculations, the active sites of benzo[α]pyrene in the mentioned cycloaddition reaction are atoms 1 and 4. It should be noted that atom 6 also shows high local nucleophilicity, but the mutual position (C17) has low nucleophilicity.

HOMO-LUMO interactions sometimes do not accurately reflect the preferred pathway for bond formation in chemical reactions because two factors control bond formation: the energy difference of the HOMO-LUMO of the reactants and the relative participation of the atomic orbitals of the active positions in the molecular orbital. HOMO orbitals do not consider the second factor. Therefore, HOMO-LUMO interactions may not always work correctly, and it can be challenging to discern when these interactions provide a reasonable description of bond formation. Recently, a powerful tool called the concept of Effective Frontier Molecular Orbitals for Reaction (FERMO) has been introduced. The FERMO concept considers a frontier molecular orbital close to the HOMO (or even the HOMO itself) in which the participation of the atomic orbitals from the active positions is maximized, thereby describing reactivity better than the HOMO. Thus, in this study, the FERMO orbital for benzo[α]pyrene was determined based on the largest contributions from atoms 1 and 4 (the active sites) [14,28].

Table 2. Values relative energies Δ*E* (kcalmol^{-1}), relative enthalpies Δ*H* (kcalmol^{-1}), relative Gibbs free energies Δ*G* (kcalmol^{-1}), and relative entropies Δ*S* (calmol^{-1}K^{-1}) obtained from the B3LYP/6-311G** method for the species involved in the reaction between fullerene C_{20} and benzo[α]pyrene.

species	Δ*E*	Δ*H*	Δ*S*	Δ*G*
C_{20}	-	-	-	-
benzo[α]pyrene	-	-	-	-
TS	6.840	7.467	-53.72	22.967
Adduct	-46.121	-43.172	-56.40	-26.292

Figure 5 shows the HOMO orbital of benzo[α]pyrene along with two other occupied orbitals close to the HOMO. As explained above, the FERMO orbital is one with an energy level of -0.2564 a.u., in which the contribution of the active site atoms (atoms 1 and 4) is maximized, allowing it to interact with the LUMO of fullerene.

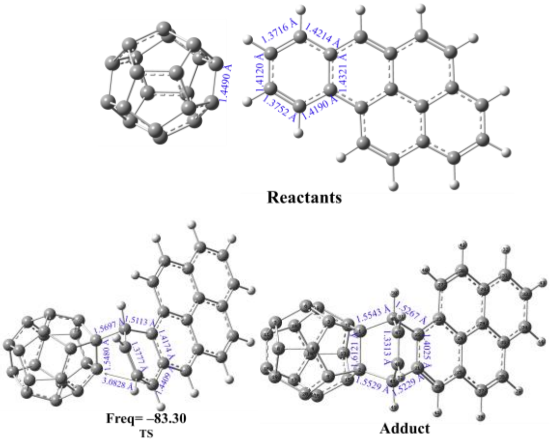

Fig. 2. Optimized structures of the reactants (fullerene C20 and benzo[α]pyrene), product, and transition state along with its imaginary frequency, obtained from B3LYP/6-311G** calculations.

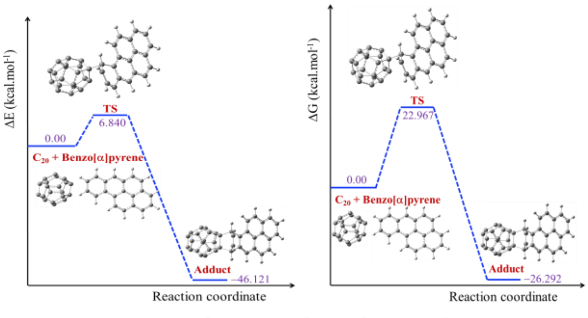

Fig. 3. Diagrams showing the relative changes in total energy and relative changes in Gibbs free energy as a function of reaction progress.

The General Electron Density Transfer (GEDT) is one of the important parameters in organic reactions. This quantity is a characteristic of transition states in cycloaddition reactions and often determines the energy barrier [29]. For this reason, this parameter was calculated for the transition state of the reaction under investigation, and the results are presented along with the electrostatic potential map of the molecule in Figure 6 (in the electrostatic potential map, red areas indicate higher electron density, while blue areas indicate lower electron density). It is worth noting that the GEDT value for fullerene C_{20} was found to be negative, whereas for benzo[α]pyrene, it was positive, indicating that during the reaction, electrons are transferred from benzo[α]pyrene to fullerene.

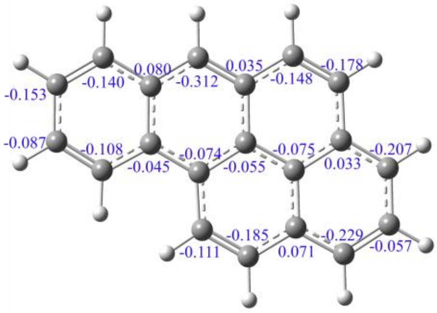

Fig. 4. Local nucleophilicity calculated for the various carbon atoms in benzo[α]pyrene.

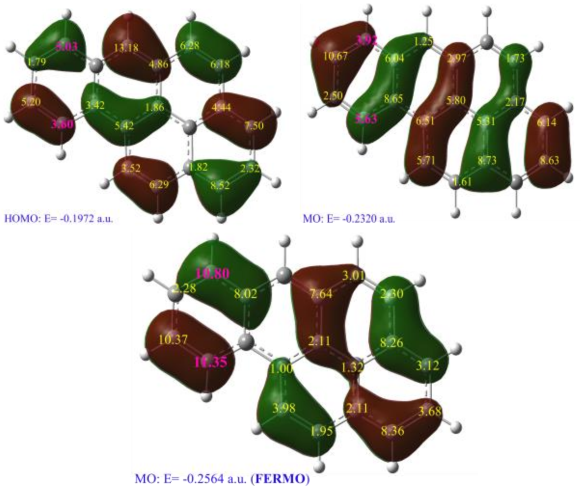

Fig. 5. Percentage of participation of various atoms in benzo[α]pyrene in frontier orbitals for determining the FERMO orbital.

Table 3. The synchronicity *Sy* calculated for the cycloaddition reactions between fullerene and benzo[α]pyrene.

parameter	$\delta_{C1\text{-}C2}$	$\delta_{C2\text{-}C3}$	$\delta_{C3\text{-}C4}$	$\delta_{C4\text{-}C'f}$	$\delta_{Cf\text{-}C'f}$	$\delta_{Cf\text{-}C1}$	δ_{Bav}	S_y
quantity	0.9544	0.3197	0.2620	0.0637	0.8892	0.9634	0.5754	0.6243

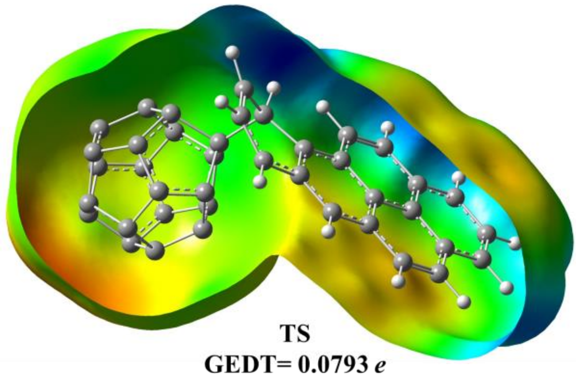

Fig. 6. Electrostatic potential map of the transition state along with the General Electron Density Transfer (GEDT).

Cycloaddition reactions often occur simultaneously. In these reactions, all bond changes happen in one step. The synchronicity parameter *Sy* can be suitable for examining these changes; therefore, the level of synchronicity *Sy* for the cycloaddition reaction under investigation was determined. It should be noted that the value of this parameter for fully synchronous reactions is equal to 1, and the further its value is from 1, the less synchronous the reaction becomes. Table 3 shows the corresponding values for this parameter in the reaction between benzo[α]pyrene and fullerene. As the results of this table indicate, the synchronicity of the reaction is relatively low. In fact, the formation of one bond between benzo[α]pyrene and fullerene occurs more rapidly than the formation of the other bond in the transition state. The results from this table, as well as the optimized structure of the transition state (Figure 2), suggest that the C4-C_f bond forms faster than the C1-Cf bond (where C_f refers to the carbon atom in fullerene).

Conclusions

Benzo[α]pyrene, a polycyclic aromatic hydrocarbon found in the atmosphere as a product of incomplete fossil fuel combustion, is recognized as a carcinogen. This study explores the potential deactivation of benzo[α]pyrene through its reaction with C_{20} fullerene using quantum computational methods. To investigate this subject, we calculated the thermodynamic and kinetic parameters for the [4+2] reaction between benzo[α]pyrene and fullerene. The findings indicate that the reaction is thermodynamically favorable, characterized by negative enthalpy and free energy values. Kinetically, the reaction proceeds with a rate constant of 9.24×10^{-5} s^{-1} at 25°C. Utilizing Fukui functions, we identified the active sites on benzo[α]pyrene for the reaction. Additionally, we determined the effective orbital for the reaction, FERMO, found at an energy level of -0.2564 a.u., where the contributions from the active site atoms (1 and 4) are maximized, allowing interaction with the fullerene LUMO orbital. General Electron Density Transfer (GEDT) calculations revealed that an electron is transferred from benzo[α]pyrene to fullerene in this reaction, exhibiting some polar characteristics. Finally, the analysis of reaction synchrony showed a low level of synchrony, indicating that the formation of two bonds between fullerene and benzo[α]pyrene in the transition state occurs at different stages.

References

[1] Gelboin H. V., Benzo[α]pyrene metabolism, activation, and carcinogenesis: role and regulation of mixed-function oxidases and related enzymes. ***Physiological Reviews,*** **1980**, 60, 1107–1166.
https://doi.org/10.1152/physrev.1980.60.4.1107

[2] Wen S., Zhao J., Sheng G., Fu J., Peng P., Photocatalytic reactions of pyrene at TiO_2/water interfaces, ***Chemosphere***, **2003**, 50, 111–119.
https://doi.org/10.1016/S0045-6535(02)00420-4

[3] Cormro A., Lib-do V., Cbiiccbio U., Pistar V., 1,3-Dipolar cycloaddition reactions of polycyclic aromatic hydrocarbons with 3,5-dichloro-2,4,6-timethyl- and 2,4,6-trimethylbenzonitrile oxide, ***Tetrahedron***, **1996**, 52, 13027–13034.

[4] Smith M. B., March J., *March's Advanced Organic Chemistry*, Wiley Interscience, New York, **2001**, pp. 1062–1076.

[5] Sikes P., *A Guidebook to Mechanism in Organic Chemistry*, Longman, Harlow, **1998**, pp. 349–351.

[6] Wilson S. R., *Nanomedicine: Fullerene and Carbon Nanotube Biology*, Kluwer Academic, Dordrecht, **2002**.
https://doi.org /10.1007/0-306-47621-5_14

[7] Brabec C. J., Sariciftci N. S., Hummelen J. C., Plastic solar cells, ***Advanced Functional Materials***, **2001**, *11*, 15.
https://doi.org/10.1002/1616-3028(200102)11:1<15:: AID - ADFM15 > 3.0.CO; 2-A

[8] Wang G. W., Chen Z. X., Muratac Y., Komatsuc K., [60] Fullerene adducts with 9-substituted anthracenes:

mechanochemical preparation and retro Diels-Alder reaction, ***Tetrahedron***, **2005**, 61, 4851–4856. https://doi.org/10.1016/j.tet.2005.02.089

[9] Prinzbach H., Weiler A., Landenberger P., Wahl F., Wörth J., Scott L.T., ***Nature***, **2000**, 407, 60. https://doi.org/10.1038/35024037

[10] Prinzbach H., Wahl F., Weiler A., Landenberger P., Woerth J., Scott L.T., ***Chemistry: European Journal***, **2006**, 12, 6268. https://doi.org/10.1002/chem.200501611

[11] Cheng X., Kan A. T., Tomson M. B., Naphthalene adsorption and desorption from aqueous C_{60} fullerene, ***Journal of Chemical & Engineering Data***, **2004**, 49, 675–683. https://doi.org/10.1021/je030247m

[12] Sarova G. H., Berberan-Santos M. N., Kinetics of the Diels-Alder reaction between C_{60} and acenes, ***Chemical Physics Letters***, **2004**, *397*, 402–407. https://doi.org/10.1016/j.cplett.2004.09.005

[13] Peyghan A. A., Noei M., DFT study on [4+2] and [2+2] cycloadditions to [60] fullerene, ***Chemical Papers***, **2014**, 68, 409–416. https://doi.org/10.2478/s11696-013-0448-z

[14] Soleymani M., Dashti Khavidaki H., Inactivation possibility of pyrene by C_{20} fullerene via cycloaddition reactions: A theoretical study, ***Computational and Theoretical Chemistry***, **2017**, 1112, 37–45. https://doi.org/10.1016/j.comptc.2017.04.014

[15] Soleymani M., Theoretical study of the possibility of functionalization of C_{20} fullerene with the simplest ketene CH_2CO, ***Journal of Structural Chemistry***, **2019**, 60, 524-535. https://doi.org/10.1134/S0022476619040036

[16] Soleymani M., Dashti Khavidaki H., Functionalization of the C_{20} fullerene by pyridine and pyrimidine: A theoretical study, ***Iranian Chemical Communication***, **2020**, 8, 111-122.

[17] Frisch M. J., Trucks G. W., Schlegel H. B., Scuseria G. E., Robb M. A., Cheeseman J. R., Scalmani G., Barone V., Mennucci B., Petersson G. A., Nakatsuji H., Caricato M., Li X., Hratchian H. P., Izmaylov A. F., Bloino J. Zheng, G., Sonnenberg J. L., Hada M., Ehara M., Toyota K., Fukuda R., Hasegawa J., Ishida M., Nakajima T., Honda Y., Kitao O., Nakai H., Vreven T., Montgomery Jr. J. A., Peralta J. E., Ogliaro F., Bearpark M., Heyd J. J. Brothers, E., Kudin K. N., Staroverov V. N., Kobayashi R., Normand J., Raghavachari K., Rendell A., Burant J. C., Iyengar S. S., Tomasi J., Cossi M., Rega N., Millam J. M., Klene M., Knox J. E., Cross J. B., Bakken V., Adamo C., Jaramillo J., Gomperts R., Stratmann R. E., Yazyev O., Austin A. J., Cammi R., Pomelli C., Ochterski J. W., Martin R. L., Morokuma K., Zakrzewski V. G., Voth G. A., Salvador P., Dannenberg J. J., Dapprich S., Daniels A. D., Farkas Ö., Foresman J. B., Ortiz J. V., Cioslowski J., Fox D. J., Gaussian 09, Revision A.1, Gaussian Inc., Wallingford, CT, **2009**.

[18] Lee C., Yang W., Parr R. G., Development of the Colle-Salvetti correlation-energy formula into a functional of the electron density, ***Physical Reviews B***, **1988**, 37, 785–789. DOI: https://doi.org/10.1103/PhysRevB.37.785

[19] Gonzalez C., Schlegel H. B., An improved algorithm for reaction path following, ***Journal of Chemical Physics***, **1989**, 90, 2154–2161. https://doi.org/10.1063/1.456010

[20] Eyring H., The activated complex in chemical reactions, ***Journal of Chemical Physics***, **1935**, 3, 107–115. https://doi.org/10.1063/1.1749604

[21] Lecea B., Arrieta A., Roa G., Ugalde J. M., Cossio F. P., Catalytic and solvent effects on the cycloaddition reaction between ketenes and carbonyl compounds to from 2-oxetanones, ***Journal of the American Chemical Society***, **1994**, 116, 9613–9619. https://doi.org/10.1021/ja00100a028

[22] Reed A. E., Curtiss L. A., Weinhold F., Intermolecular interactions from a natural bond orbital, donor-acceptor viewpoint, ***Chemical Reviews***, **1988**, 88, 899-926. https://doi.org/10.1021/cr00088a005

[23] Parr R. G., Szentpaly L. V., Liu S., Electrophilicity index, ***Journal of the American Chemical Society*, 1999**, 121,1922–1924. https://doi.org/10.1021/ja983494x

[24] Geerlings P., Proft F. De, Langenaeker W., Conceptual Density Functional Theory, ***Chemical Reviews*, 2003**, 103, 1793-1874. https://doi.org/10.1021/cr990029p

[25] Yang W., Mortier W. J., The use of global and local molecular parameters for the analysis of the gas-phase basicity of amines, ***Journal of the American Chemical Society*, 1986,** 108, 5708-5711. https://doi.org/10.1021/ja00279a008

[26] Domingo L. R., Aurell M. J., Pêrez P., Contreras R., Quantitative characterization of the local electrophilicity of organic molecules, Understanding the regioselectivity on Diels-Alder reactions, ***Journal of Physical Chemistry A***, **2002**, 106, 6871-6875. https://doi.org/10.1021/jp020715j

[27] Pêrez P., Domingo L. R., Duque-Noreňa M., Chamorro E., A condensed-to-atom nucleophilicity index. An application to the director effects on the electrophilic aromatic substitutions, ***Journal of Molecular Structure THEOCHEM*, 2009**, 895, 86-91. https://doi.org/10.1016/j.theochem.2008.10.014

[28] La Porta F. A., Ramalho T. C., Santiago R. T., Rocha M. V. J., da Cunha E. F. F., Orbital signatures as a descriptor of regioselectivity and chemical reactivity: the

role of the frontier orbitals on 1,3-dipolar cycloadditions, ***Journal of Physical Chemistry A*, 2011**, 115, 824–833. https://doi.org/10.1021/jp108790w

[29] Domingo L. R., A new C-C bond formation model based on the quantum chemical topology of electron density, ***RSC Advances***, **2014**, 4, 32415-32428. DOI: 10.1039/C4RA04280H